In Kr, the two-electron excitation series for which some evidence has been established appear in Tabie III. Similarly, such series in Xe, are given in Table IV. The average quantum defect $(n-n^*)$ for the observed members to the indicated limits is also given.

CONCLUSIONS

The two-electron resonances listed into series for Kr and Xe represent only one-fourth of those cataloged. The principle problem is, of course, the complicated configuration interactions present which displace the levels from locations expected from simple theoretical considerations and produce intensity anomalies. For some series the profiles of the resonances vary with the principle quantum number. Other series appear fragmentarily, having observable strength only where they have borrowed sufficient intensity from an interacting configuration. As a result of these difficulties it appears at present that substantial theoretical calculations are required to analyze the spectra further. Prints of the spectra are available from the authors, and the reader is again reminded that the detailed lists are available in Ref. 9.

---

*Present address: University of Reading, Physics Department, J. J. Thomson Physical Lab., White Knights Park, Reading, Berkshire, England.

[1]R. P. Madden and K. Codling, Phys. Rev. Letters 10, 516 (1963).

[2]R. P. Madden and K. Codling, J. Opt. Soc. Am. 54, 268 (1964); K. Codling and R. P. Madden, Phys. Rev. Letters 12, 106 (1964); Appl. Opt. 4, 1431 (1965).

[3]J. A. R. Samson, Phys. Letters 8, 107 (1964).

[4]R. P. Madden and K. Codling, Astrophys. J. 141, 364 (1965).

[5]K. Codling, R. P. Madden, and D. L. Ederer, Phys. Rev. 155, 26 (1967).

[6]R. P. Madden, D. L. Ederer, and K. Codling, Phys. Rev. 177, 136 (1969).

[7]D. L. Ederer, following paper, Phys. Rev. A 4, 2263 (1971).

[8]R. P. Madden, D. L. Ederer, and K. Codling, Appl. Opt. 6, 31 (1967).

[9]K. Codling and R. P. Madden, J. Res. Natl. Bur. Std. 76A, 1 (1972).

[10]The direction of asymmetry is indicated in Ref. 9 by giving the sign of "q" as defined by U. Fano and J. W. Cooper, Phys. Rev. 137, A1364 (1965).

[11]J. A. R. Samson, in *Advances in Atomic and Molecular Physics*, edited by D. R. Bates and I. Estermann (Academic, New York, 1966), Vol. 2, p. 177.

[12]M. Mansfield, Ph.D. thesis (Imperial College, London, 1970) (unpublished).

[13]C. E. Moore, *Atomic Energy Levels*, Natl. Bur. Std. (U.S.) Circ. No. 467 (U.S. GPO Washington, D.C., 1949), Vol. I.

[14]L. Minnhagen (private communication).

PHYSICAL REVIEW A VOLUME 4, NUMBER 6 DECEMBER 1971

Cross-Section Profiles of Resonances in the Photoionization Continuum of Krypton and Xenon (600–400 Å)

David L. Ederer
National Bureau of Standards, Washington, D. C. 20234
(Received 16 July 1971)

The cross-section profiles in krypton and xenon have been measured for one- and two-electron excitations of the type $ns^2np^6(^1S_0) \rightarrow nsnp^6(^2S_{1/2})mp$ or $ns^2np^6(^1S_0) \rightarrow ns^2np^4(^3P, {}^1D, {}^1S)mlm'l'$. These cross sections were assumed to have the form

$$\sigma(E) = C(E) + \sum_i \frac{(E-E_i)(\Gamma_i/2)a_i + (\Gamma_i/2)^2 b_i}{(E-E_i)^2 + (\Gamma_i/2)^2},$$

where the adjustable parameters $C(E)$, b_i, a_i, E_i, and Γ_i were determined by a least-squares unfolding process which separated the smearing effect of the monochromator slit from the true optical density. Parameter values and cross-section curves are given for 12 krypton resonances and 11 xenon resonances.

I. INTRODUCTION

Photoionization in noble gases and metallic vapors has been the object of a great deal of experimental and theoretical attention[1] recently. Experimentally, the noble gases have several distinct advantages over metallic vapors in that they are easy to handle, noncorrosive, and monoatomic. Theoretically, their strategic location throughout the periodic table is ideal for a systematic study of the photoionization process.

The development of continuum light sources[2] paved the way to the study of discrete excitation states lying in the photoionization continua of

atoms. These excitation states, by virtue of their interaction with adjacent photoionization continua, produce asymmetric structure in the photoionization cross section. A large number of gases and solids exhibiting these discrete excitation features have been studied.[3-5] An extensive study of helium,[6] neon,[7] and argon[8] has been reported, as well as a preliminary study of excitations in krypton and xenon.[9] The preceding paper[10] is an extension of the earlier results in krypton and xenon presenting wavelength positions and some analysis of all the observed one- and two-electron resonance states lying between the lowest ionization limits and the inner d shell excitations. The purpose of this paper is to present measurements of the photoionization cross section in the vicinity of some one- and two-electron excitation resonances in krypton and xenon supplementing measurements of the continuum photoionization cross section of krypton and xenon that have been made[11,12] with line sources.

We chose to study resonances associated with $ns^2np^6(^1S_0) - nsnp^6(^2S_{1/2})mp$ Rydberg series in krypton and xenon and the lowest-energy two-electron excitations of the type $ns^2np^6(^1S_0) - ns^2np^4mlm'l'$ because the prominence and width of these resonances made it feasible to determine the parameters that describe their cross-section profile and because these resonances are more tractable from a theoretical standpoint.

II. EXPERIMENTAL

The NBS 180-MeV synchrotron[13] provided the continuum source of radiation used in performing these absorption measurements, and a 3-m grazing-incidence monochromator[14] with 12-μm slits (equivalent spectral bandpass, 0.067 Å) provided the transmission scans. The gas was admitted directly into the monochromator and was confined to a region between the entrance and exit slits. A precision oil manometer[15] was used to measure the pressure over a range 5×10^{-3}–100×10^{-3} Torr.

The photon beam transmitted by the gas was detected by a crossed electric and magnetic field photoelectron multiplier with a tungsten photocathode. The counting rate for this detector without the absorbing gas was typically 500 sec.$^{-1}$ A second detector sensitive to the visible synchrotron radiation was used to provide a continuous normalization for the transmission measurements by monitoring the number of electrons accelerated during each machine cycle. The exit slit and detector combination was scanned continuously during data acquisition at a rate of 0.15 or 0.40 Å/min over a wavelength interval of up to 10 Å.

III. DATA REDUCTION

A digital computer was used to facilitate the analysis of the transmission data. For each resonance group normalized spectrum scans for several pressures were recorded on chart paper and digitized so that each resonance feature contained at least 50 data points. Background radiation, consisting of multiple-order diffracted radiation and of radiation scattered by the grating, was subtracted from the raw transmission data in the initial phase of the computation. The intensity of this extraneous radiation was determined by the technique described in Ref. 8 and comprised approximately 3% of the total radiation detected in the wavelength range 500–600 Å.

The optical bandpass is comparable to the width of some of the observed resonances; therefore, the measured transmission profile of these resonances is modified by the slit function. The following data reduction procedure was devised[16] to account for this modification by the slit function. A trial transmission was first computed from a parametrized model cross section and then smeared by the slit function. This model transmission spectrum was compared with the data and the parameters determining the spectral shape of the cross section were adjusted until a best least-squares fit to the data was obtained.

The trial transmission $P(E_i)$ at the ith data point is given by

$$P(E_i) = W(E_i) \star [T(E_i)] , \tag{1}$$

where the star in Eq. (1) denotes a convolution integral of the monochromator window function $W(E)$ and the unsmeared calculated transmission $T(E)$. A window function of Gaussian form[17] was used in the computation of the convolution integral. The integral was approximated by a 14-interval numerical integration extending over an energy range corresponding to three slit widths.

The transmission is related to the photoionization cross section by the following equation:

$$T(E) = e^{-n l \sigma(E)} , \tag{2}$$

where n is the atom number density and l is the optical path length in the gas. The cross section $\sigma(E)$ can be parametrized mathematically in several different ways.[18,19] Although the formal approach to each parametrization is quite different, their theoretical equivalence has been demonstrated.[20] A cross section parametrized according to Shore[19] was used to analyze resonance structure in Ca I[21] and Sr I.[22] In Zn I[23] the resonance structure due to the excitation $3d^{10}4s^2 - 3d^9 4s^2 4p$ was fitted equally well by either the parametrization of Mies[18] or Shore.[19] Because of its mathematical simplicity, Shore's parametrization, expressed as

$$\sigma(E) = C(E) + \sum_i^N \frac{(E - E_i)(\Gamma_i/2)\, a_i + (\Gamma_i/2)^2 b_i}{(E - E_i)^2 + (\Gamma_i/2)^2} , \tag{3}$$

was chosen for this analysis. In Eq. (3), a_i, b_i have the dimension of a cross section and are proportional to products of dipole and Coulomb matrix elements connecting the ground state with the continuum and the discrete excited state. In this discussion the adjustable parameters Γ_i, the resonance width, E_i, the resonance energy position, and $C(E)$, the total background cross section, as well as a_i and b_i, are assumed independent of the photon energy E. It should be noted as $a_i \to 0$ each term in the sum reduces to a simple Lorentzian profile. In this case b_i is proportional to the oscillator strength between the ground state and the ith excited state and is inversely proportional to resonance width Γ_i.

For an isolated resonance, Eq. (3) reduces to the familiar Fano[24,25] parametrization

$$\sigma(E) = C(E) + \frac{\sigma_a q (\Gamma/2)(E - E_r) + \sigma_a (q^2 - 1)(\Gamma/2)^2}{(E - E_r)^2 + (\Gamma/2)^2} . \tag{4}$$

The quantity σ_a is the background cross section associated with the fraction of the available continua with which the discrete state interacts, σ_b is the remaining background cross section, and q is the profile index, while the total continuum background cross section $C(E)$ is given by $C(E) = \sigma_a + \sigma_b$.

A quantity of theoretical importance is the correlation index[25] ρ which is a measure of the projection of the final continuum-state vector (after autoionization) upon the continuum-state vector representing all dipole transitions from the ground state. For resonances that are described by Eq. (4) we have $\rho^2 = \sigma_a / C(E)$, but a more general definition[18] that applies to overlapping resonances is given by

$$\rho_n^2 = (\textstyle\sum_\beta \upsilon_{n,\beta}\, t_\beta^c)^2 / (\sum_\beta \upsilon_{n,\beta}^2)(\sum_\beta t_\beta^{c2}) , \tag{5}$$

where $\upsilon_{n,\beta}$ is the configuration matrix element between an excited autoionizing state n and a continuum channel β, and t_β^c is the dipole matrix element connecting the ground state with a continuum channel β. For the outer p electrons of the rare gases there is a partial photoionization cross section $\sigma_\beta = |t_\beta^c|^2$ into each of the five allowed $J = 1$ continua and each autoionizing state has a partial width $\Gamma_{n,\beta} = 2\pi |\upsilon_{n,\beta}|^2$ associated with these continua.

Photoionization measurements yield information about the total width $\Gamma_n = 2\pi(\sum_\beta \upsilon_{n,\beta}^2)$ and the total cross section $C(E) = (\sum_\beta t_\beta^{c2})$, while photoelectron spectroscopy measurements[26] give some details about the partial widths and cross sections. However, it is clear that the angular dependence of the photoelectron energy distribution and its variation through the resonance region will be essential additional information for the complete determination of the partial widths and cross sections.

The analysis of the data was divided into separate energy intervals that included the four lowest members of resonances belonging to the $4s^2 4p^6(^1S_0) \to 4s4p^6(^2S_{1/2})np$ series in krypton and $5s^2 5p^6(^1S_0) \to 5s5p^6(^2S_{1/2})np$ series in xenon as well as resonances due to the lowest-energy two-electron excitations. The decision to treat resonances in a particular energy interval as a group according to Eq. (3) or to treat them as single noninteracting resonances according to Eq. (4) was based on the author's judgment of how great an effect the presence of a resonance had on its neighbors. With the number of resonances for a given region fixed, initial values for the parameters (C, a_i, b_i, Γ_i, E_i) were chosen and the model transmission was computed according to Eq. (1) at each data point. A nonlinear least-squares[27] parameter-fitting computer algorithm fitted the model transmission to the data by adjusting the value of each parameter until the fractional change of each parameter from one iteration to the next was less than 0.001. At this point the search for the best fit was terminated and a confidence limit calculation estimated the variance of the parameters. Typically the rms deviation of the observation from the "best" model transmission curve was 0.004 for values of the transmission that ranged between 0.05 and 0.8.

IV. RESULTS

The weighted average[28] of each parameter and its standard deviation for the krypton and xenon resonance profiles are presented in Table I and Table II, respectively. The code number and wavelengths listed in Tables I and II are taken from Ref. 10 and the energy E listed in the third column is computed from these wavelengths. If several resonances are analyzed as a group the energy position of one of them is fixed (indicated by 0.0 in the ΔE column) and the energy difference ΔE between it and other members of the group is derived from the computed values of E_i in Eq. (3). The quantities a, b, C, and Γ are defined by Eq. (3) and are the parameters that represent each resonance using Shore's[19] representation. If the resonance was analyzed under the assumption that it was a single noninteracting resonance,[29] the values of q and ρ^2 listed in the tables were obtained by evaluating q and ρ^2 for each spectral scan and then finding the mean and standard deviation in the usual manner.

The number in the last column indicates how many spectral scans were analyzed to obtain the parameter values, while the bracket in the last column encloses the number of resonances analyzed as a group.

In addition to the random error cited in Tables I and II, an additional source of systematic error is present in the parameters a, b, and Γ (and also in q and ρ^2) due to the uncertainty (± 0.006 Å) in the spectral width of the slit function. The magnitude

TABLE I. Parameters for resonances in krypton. The quantities a, b, C, Γ, and ΔE define the resonance profile according to Eq. (3), while the profile index q and the correlation index ρ^2 are evaluated when the resonance was treated as a single noninteracting resonance. The bracket in the number-of-runs column encloses the number of resonances included in the group analyzed.

Code[a]	λ (Å)	E (eV)	ΔE (meV)	b (cm^{-1})	a (cm^{-1})	C (cm^{-1})	Γ[b] (meV)	q	ρ^2	No. of runs
1	501.23	24.735	···	−260 ± 80	−60 ± 15	815 ± 70	4.0 ± 0.5	−0.22 ± 0.03	0.34 ± 0.03	4
3			67.0 ± 0.6[c]	−450 ± 55	280 ± 60		19.04 ± 0.54			
4			38.9 ± 0.03	−500 ± 45	0 ± 40	750 ± 70	7.50 ± 0.70			7
5	496.07	24.992	0.0	−430 ± 45	−300 ± 70		22.8 ± 0.8			
6	492.52	25.173	···	−295 ± 75	−30 ± 12	770 ± 90	3.9 ± 0.3	−0.10 ± 0.06	0.39 ± 0.02	3
9	472.26	26.253	0.0	−60 ± 120	350 ± 150		1.58 ± 0.28			
10			44.4 ± 0.4	−220 ± 100	320 ± 20	680 ± 70	7.36 ± 0.80			8
11			55.3 ± 2.5	−515 ± 65	−150 ± 85		13.2 ± 0.5			
14	462.71	26.794	···	−385 ± 80	45 ± 15	635 ± 60	7.8 ± 0.6	0.11 ± 0.03	0.62 ± 0.02	5
15	461.83	26.864	···	−132 ± 80	−55 ± 20	635 ± 60	3.5 ± 0.8	−0.38 ± 0.06	0.24 ± 0.03	3
18		27.036	42.0 ± 1.5	−55 ± 30	130 ± 15	650 ± 50	6.8 ± 0.8			7
19	457.86	27.078	0.0	−105 ± 40	−370 ± 25		7.18 ± 0.32			

[a]The code number and the wavelength are taken from Ref. 10.

[b]In addition to the statistical error quoted, the parameters a, b, Γ, q, and ρ^2 are subject to a systematic error due to the uncertainty in the width of the slit function (3.0 ± 0.3 meV). This systematic error amounts to approximately 10% of the parameter value for resonances whose width is equal to the slit function width and decreases proportionately as the slit width to resonance width ratio decreases.

[c]The quoted error for the parameters of these resonances corresponds to the standard deviation.

of this error[16] depends on the width of the resonance compared to the slit width. In this investigation a number of resonances were approximately as wide as the slit function,[30] and the width of the sharpest resonance studied was about a factor of 2 smaller than the slit function. For resonances of these widths the systematic error attributable to the uncertainty in the width of the window function is estimated to add an additional 10% of the parameter value to the statistical uncertainties listed in Tables I and II. As the width of the resonance increases with respect to the width of the slit function, this systematic error decreases proportionately.

The curves for the krypton and xenon cross section shown, respectively, in Figs. 1 and 2 were computed from the parameters listed in Tables I and II. A background cross section decreasing linearly for increasing photon energies was used in computing the cross-section curves in Figs. 1

TABLE II. Parameters for resonances in xenon. The quantities a, b, C, Γ, and ΔE define the resonance profile according to Eq. (3). The profile index q and the correlation index ρ^2 are evaluated when a resonance is treated as a single noninteracting resonance. The bracket in the last column encloses the resonances analyzed as a group.

Code[a]	λ (Å)	E (eV)	ΔE (meV)	b (cm^{-1})	a (cm^{-1})	C (cm^{-1})	Γ[b] (meV)	q	ρ^2	No. of runs
1	599.99	20.664		−550 ± 40[c]	26 ± 20	790 ± 60	3.7 ± 0.4	0.03 ± 0.03	0.70 ± 0.04	6
2	595.93	20.805		−270 ± 15	−70 ± 15	720 ± 30	8.14 ± 0.8	−0.24 ± 0.03	0.40 ± 0.02	7
3	591.77	20.951		−485 ± 60	115 ± 15	760 ± 60	31.2 ± 0.8	0.23 ± 0.04	0.65 ± 0.03	6
4	589.54	21.030		−350 ± 40	−55 ± 15	740 ± 50	14.6 ± 0.8	−0.14 ± 0.04	0.50 ± 0.04	5
9	579.16	21.407		−230 ± 15	−120 ± 30	680 ± 55	5.8 ± 0.6	−0.32 ± 0.13	0.41 ± 0.03	4
10	570.79	21.721		−80 ± 25	−60 ± 10	715 ± 70	7.2 ± 1.0	−0.50 ± 0.20	0.19 ± 0.05	5
16	557.83	22.226		−405 ± 25	65 ± 8	620 ± 35	13.0 ± 0.6	0.16 ± 0.04	0.67 ± 0.02	7
27	546.08	22.704		−420 ± 55	90 ± 18	600 ± 60	6.25 ± 0.3	0.21 ± 0.02	0.65 ± 0.04	6
34	540.62	22.933	0.0	75 ± 40	−125 ± 35	605 ± 45	4.2 ± 1.3			5
35			8.5 ± 0.8	−95 ± 45	130 ± 35		10.0 ± 1.4			
36	539.33	22.988		10 ± 30	−100 ± 25	550 ± 45	3.6 ± 1.1	−1.05 ± 0.10	0.18 ± 0.05	5

[a]The code numbers and wavelengths are taken from Ref. 10.

[b]In addition to the statistical error quoted, the parameters a, b, Γ, and ρ^2 are subject to a systematic error due to the uncertainty in the width of the slit function (2.0 ± 0.2 meV). This systematic error amounts to approximately 10% of the parameter value for resonances whose width is equal to the slit function width and decreases proportionately as the slit width to resonance width ratio decreases.

[c]The quoted error for the parameters of these resonances correspond to 1 standard deviation.

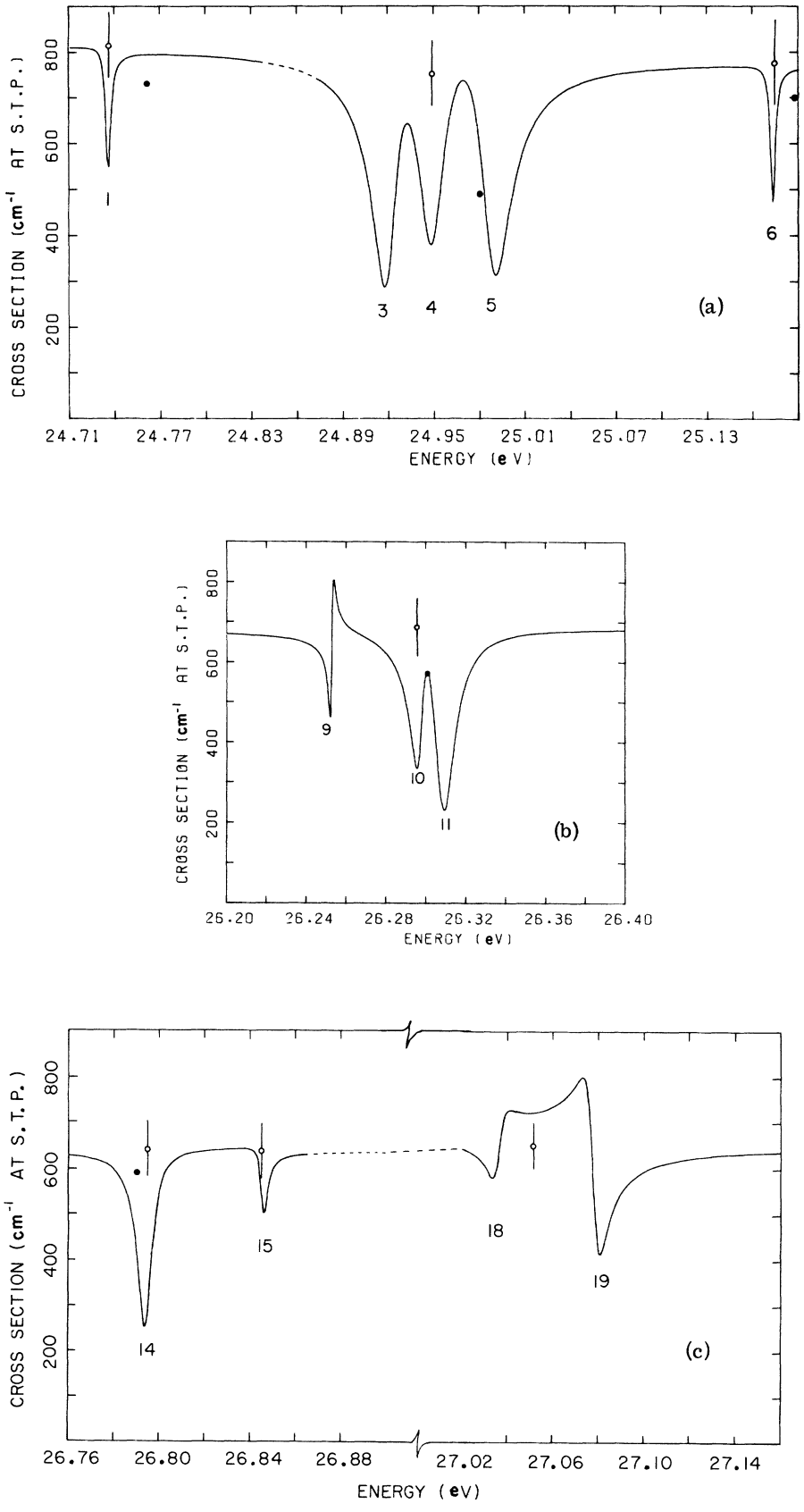

FIG. 1. Photoionization cross section of krypton calculated from the parameters listed in Table I, according to Eq. (3) in the text. The cross section for resonances in the vicinity of the $n=5$ member of the $4s^2 4p^6 ({}^1S_0) \rightarrow 4s4p^6 ({}^2S_{1/2})\, np$ series is shown in (a), while resonances near the $n=6$ series member are shown in (b), and (c) illustrates the cross section near the $n=7$ and 8 members of this series. For this presentation the background cross section decreases linearly with increasing photon energy. The resonances are identified by the code numbers of Ref. 10. The value of the background cross section C determined for each resonance or group of resonances is denoted by O; the magnitude of one standard deviation is indicated by the vertical bars. The symbol ● denotes data from Ref. 11. A dashed line indicates a spectral region containing resonances that were not analyzed.

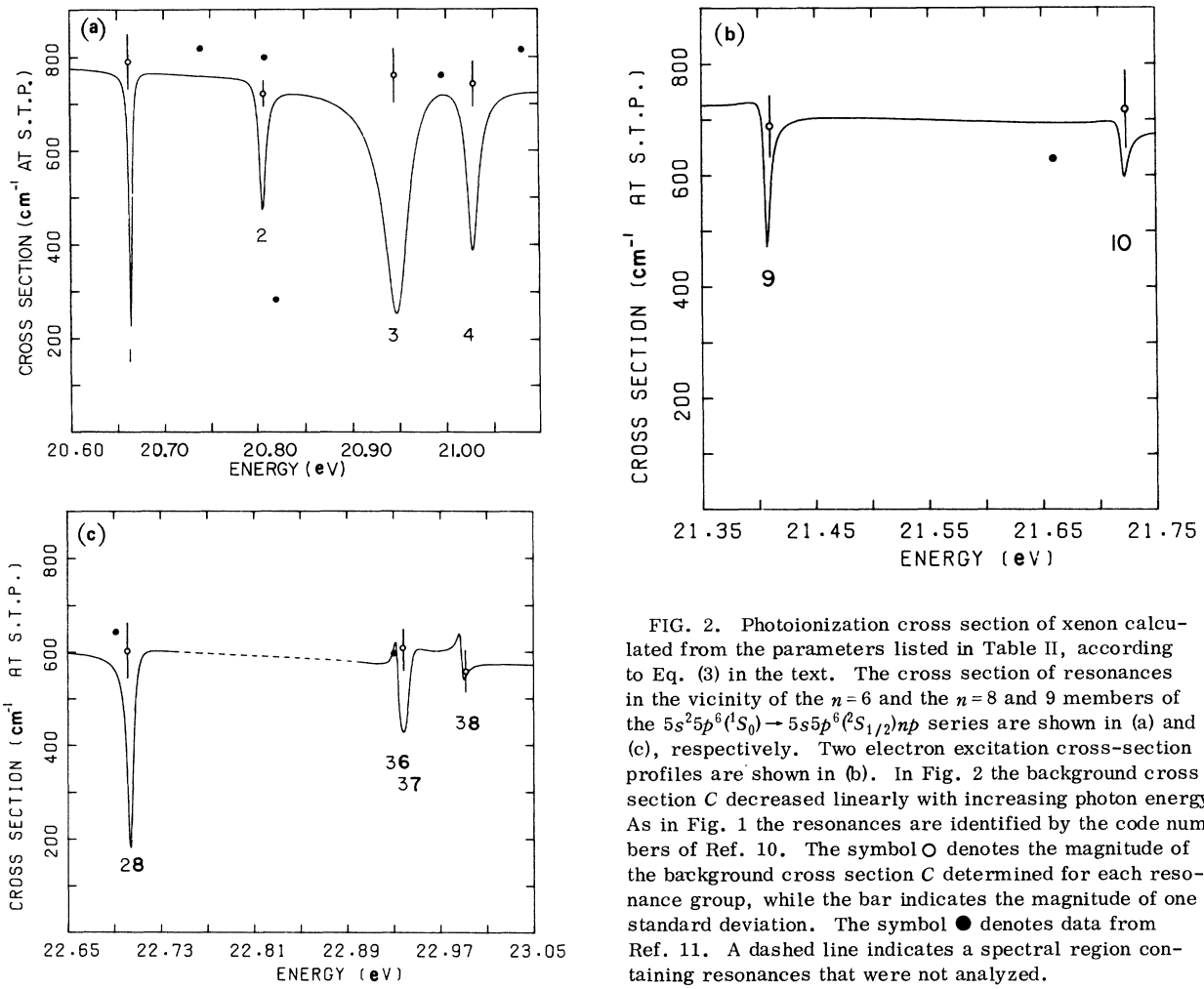

FIG. 2. Photoionization cross section of xenon calculated from the parameters listed in Table II, according to Eq. (3) in the text. The cross section of resonances in the vicinity of the $n = 6$ and the $n = 8$ and 9 members of the $5s^2 5p^6(^1S_0) \rightarrow 5s5p^6(^2S_{1/2})np$ series are shown in (a) and (c), respectively. Two electron excitation cross-section profiles are shown in (b). In Fig. 2 the background cross section C decreased linearly with increasing photon energy. As in Fig. 1 the resonances are identified by the code numbers of Ref. 10. The symbol O denotes the magnitude of the background cross section C determined for each resonance group, while the bar indicates the magnitude of one standard deviation. The symbol ● denotes data from Ref. 11. A dashed line indicates a spectral region containing resonances that were not analyzed.

and 2, where the average slope of the background cross section as a function of photon energy was determined from the continuum cross-section data of Ref. 11 in the region of these resonances. In the analysis of the data the background cross section was assumed constant; however, the wings of the widest resonance effectively extend about 50 meV to either side of the resonance center, and the total change in the linearly decreasing background cross section over this energy range is approximately 10 cm^{-1}. A change in the background cross section of this magnitude would introduce in the parameters an error small compared to their statistical uncertainty which becomes even smaller for sharper resonances.

In Figs. 1 and 2 the values of the continuum cross-section data measured at discrete wavelengths by Samson[11] are denoted by the solid circles. The value of the background continuum cross section at the center of the resonance (the quantity C in Tables I and II) determined from the present measurements is denoted by the open circles whose bars have a magnitude of one standard deviation. In Figs. 1 and 2 all the resonances shown are identified by the code numbers of Ref. 10, and a dashed region indicates an energy interval containing resonances where the cross section was not evaluated.

V. DISCUSSION

At most two of the resonances shown in Fig. 1(a) can be associated with the $4s^2 4p^6(^1S_0) - 4s4p^6(^2S_{1/2})np$ single-electron excitation series in krypton.[10] The other resonances are likely first members of series converging to $4p^4(^3P)5s(^{2,4}P)$ terms in Kr II.

The resonances near the second member of the $4s^2 4p^6(^1S_0) - 4s4p^6(^2S_{1/2})np$ series are shown as the center plot, Fig. 1(b), while the lower curve, Fig. 1(c), is the absorption cross section in the vicinity of the third and fourth members of this one-electron excitation series.

The cross section in the vicinity of the first

member of the $5s^2 5p^6(^1S_0) - 5s5p^6(^2S_{1/2})np$ series in xenon is shown in Fig. 2(a). As in krypton, at most two of the resonances can be associated with the series corresponding to the excitation of a single electron. The other resonances and resonances 9 and 10 in Fig. 2(b) must be associated with two-electron excitation states. The second member of the $5s^2 5p^6(^1S_0) - 5s5p^6(^2S_{1/2})np$ series is not shown, but the third and fourth members of this single-electron excitation series are shown in Fig. 2(c). All the xenon resonances with the exception of 34 and 35 were treated in the approximation of isolated resonances.

In Fig. 1 the resonances numbered 3, 11, 14, and 19 correspond to the first four members of the $4s^2 4p^6(^1S_0) - 4s4p^6(^2S_{1/2})np$ one-electron excitation series. In Fig. 2 the resonances 3, 16, 27, and 34 are associated[31] with the $n = 6$, 7, 8, and 9 members of the corresponding $5s^2 5p^6(^1S_0) - 5s5p^6 \times (^2S_{1/2})np$ excitation series in xenon.

For neon[7] and argon,[8] two-electron excitation states are sufficiently separated in energy from the one-electron excitation series that the overlap is negligible and the ratio $R = 1 - \sigma_{min}/C(E)$, where σ_{min} is the minimum cross section in the resonance, is equal to ρ^2. In the case of krypton and xenon, the two-electron excitation states overlap the single-electron excitation series; consequently, although R still suggests a measure of the interaction of these resonances with the continuum, it is not necessarily equal to ρ^2. For this reason the prominence of the single-electron excitation series and some of the two-electron excitation states is a result of the strong interaction of the resonance with the available continuum channels. In Table III, R is evaluated from the cross section shown in Figs. 1 and 2 for selected Kr and Xe resonances identified by the code number. The principal quantum number n, the effective quantum number n^*, and the product $(n^*)^3\Gamma$ are also given in this table.

TABLE III. Code, cross-section ratio R (described in text), principal quantum number n, effective quantum number n^*, and the product of n^{*3} and the width Γ of selected resonances in krypton and xenon.

Code	R	n	n^*	$(n^*)^3\Gamma$ (eV)
		Krypton		
3	0.63			
4	0.52			
5	0.61	5	2.323	0.28
10	0.53			
11	0.66	6	3.363	0.50
14	0.60	7	4.351	0.64
18	0.37	8	5.303	1.01
		Xenon		
1	0.70			
2	0.38			
3	0.67	6	2.359	0.41
4	0.48			
16	0.67	7	3.409	0.51
27	0.68	8	4.433	0.54
34	0.27	9	5.420	0.67

For an unperturbed Rydberg series q, ρ^2, and the product $(n^*)^3\Gamma$ should be constant or smoothly varying.[25] In neon[7] and argon[8] the first few members of the single-electron excitation series involving the s subshell electron exhibited these properties. The corresponding resonances in krypton and xenon behave in a more complicated way because of the configuration interaction between the single-electron excitation series and two-electron excitations. Although the quantum defect of the one-electron excitation series is approximately constant[10] for each series, the product $(n^*)^3\Gamma$ changes significantly. Particularly in krypton the first and fourth series members show a perturbation by neighboring resonances, while in xenon only the fourth member shows a width perturbation that is reflected in the $(n^*)^3\Gamma$ product. The perturbation that affects the $(n^*)^3\Gamma$ product of the fourth series member is also reflected in a smaller value for R. However, the value of R is constant for the lower Rydberg series members in krypton and xenon in spite of the apparent strong interaction that the first series member in krypton has with adjacent resonances.

In krypton the eight lowest-lying resonances are grouped together and have quantum defects whose magnitudes are compatible with resonances that could be reasonably associated with the lowest $J = 1$ levels belonging to series converging to $4s4p^6 \times (^2S_{1/2})$, and $4s^2 4p^4(^3P)4s(^{2,4}P)$ terms in Kr II. The assignment of these resonances can not be carried out with certainty without the theoretical guidance of a multiconfiguration *ab initio* calculation. In particular, even though resonance number 5 has been assigned to a transition of a single $4s$ electron to one of the $5p$ levels in krypton, the profile parameters and quantum defects would not exclude either of the two prominent adjacent resonances.

There are two reports[11,12] of measurements of the continuum photoabsorption cross section of krypton and xenon in this wavelength region, along with a low resolution measurement[32] of the cross-section profile in the vicinity of the krypton resonance due to $4s^2 4p^6(^1S_0) - 4s4p^6(^2S_{1/2})5p$. Although the magnitude of the background cross section is in good agreement with this work, the cross section profile is distorted due to the lower instrumental resolution. The present values of the background cross section for krypton (C in Table I) tend to be systematically higher than those of Samson[11] but somewhat lower in magnitude than the measure-

ments of Rustgi *et al.*[12] The displacements are within the limits of statistical error; however, in the case of xenon the present measurements are in better agreement with those of Samson than those of Rustgi *et al.*

In conclusion we have presented cross section measurements in the vicinity of the more prominent one- and two-electron excitation states in krypton and xenon. The smearing effect of the slit on the data was accounted for by an unfolding process based on a least-squares fit of the observations to the transmission calculated from a parametrized model folded with the slit function. The parameters describing the cross section in the vicinity of a resonance were evaluated for 12 krypton resonances and 11 xenon resonances using this data-reduction technique.

ACKNOWLEDGMENT

The author is grateful to Dr. R. P. Madden for his suggestions concerning this work and to Dr. T. Lucatorto for a critical reading of the manuscript.

[1]For a review of this work see (a) J. A. R. Samson, *Advances in Atomic and Molecular Physics* (Academic, New York, 1966), Vol. II, pp. 177–261; and (b) Geoffrey V. Marr, *Photoionization Processes in Gases* (Academic, New York, 1967).

[2]A brief review of continuum light sources can be found in Ref. 1(b), pp. 62–64.

[3]A review of this work up to 1968 can be found in U. Fano and J. W. Cooper, Rev. Mod. Phys. 40, 441 (1968).

[4]A representative selection of some of the work since then is G. V. Marr and J. M. Austin, J. Phys. B 2, 107 (1969); W. R. S. Garton and J. P. Connerade, Astrophys. J. 155, 667 (1969); R. Heppinstall and G. V. Marr, Proc. Roy. Soc. A310, 35 (1969); J. Berkowitz and C. Lifshitz, J. Phys. B 1, 438 (1968).

[5]R. Haensel, G. Keitel, C. Kunz, P. Schreiber, and B. Sonntag, in Proceedings of the Tenth European Conference on Molecular Spectroscopy, Liege, 1969 (unpublished).

[6]R. P. Madden and K. Codling, Astrophys. J. 141, 364 (1965).

[7]K. Codling, R. P. Madden, D. L. Ederer, Phys. Rev. 155, 26 (1967).

[8]R. P. Madden, D. L. Ederer, and K. Codling, Phys. Rev. 177, 136 (1969).

[9]R. P. Madden and K. Codling, J. Opt. Soc. Am. 54, 268 (1964).

[10]K. Codling and R. P. Madden, preceding paper, Phys. Rev. A 4, 2266 (1971).

[11]J. A. R. Samson, Geophysics Corporation of America, Technical Report No. 64-3-N, 1964 (unpublished).

[12]O. P. Rustgi, E. I. Fischer, and C. H. Fuller, J. Opt. Soc. Am. 54, 745 (1964).

[13]K. Codling and R. P. Madden, J. Appl. Phys. 36, 380 (1965).

[14]R. P. Madden, D. L. Ederer, and K. Codling, Appl. Opt. 6, 31 (1967).

[15]A. M. Thomas and J. L. Cross, J. Vacuum Sci. Tech. 4, 1 (1967).

[16]D. L. Ederer, Appl. Opt. 8, 2315 (1970).

[17]For this instrument the diffraction width equaled the geometrical slit width; hence a Gaussian with full width at half-maximum equal to the optical slit width was a good approximation to the slit function. See, for example, P. C. von Planta, J. Opt. Soc. Am. 47, 629 (1957).

[18]F. H. Mies, Phys. Rev. 175, 164 (1968).

[19]B. W. Shore, Phys. Rev. 171, 43 (1968).

[20]J. H. Macek and P. G. Burke (private communication).

[21]G. H. Newsom and B. W. Shore, J. Phys. B 1, 742 (1968).

[22]W. R. S. Garton, G. L. Grasdalen, W. H. Parkinson, and E. M. Reeves, J. Phys. B 1, 114 (1968).

[23]G. V. Marr and J. M. Austen, J. Phys. B 2, 107 (1969).

[24]U. Fano, Phys. Rev. 124, 1866 (1961).

[25]U. Fano, and J. W. Cooper, Phys. Rev. 137, A1364 (1965).

[26]J. A. R. Samson and R. C. Cairns, Phys. Rev. 73, 80 (1968).

[27]D. W. Marquardt, J. Soc. Indust. Appl. Math. 11, 431 (1963). The computer program entitled, "Least Squares Estimation of Non-Linear Parameters" can be obtained from the Share Distribution Library (Share Distribution No. 1428). A revised program is also available (Share Distribution No. 209 401).

[28]The weight for a parameter determined from a particular transmission scan was established from the reciprocal of the square of the standard deviation estimated in the confidence limit calculation.

[29]Catagorizing a resonance as noninteracting was a subjective decision arrived at by judging the appearance of the resonance and its proximity to neighboring resonances. Whether or not the parameters determined in this approximation could be used to give a "true" representation of the cross section in the region of the resonance was tested. The cross section was computed first in the region of the resonance using the single-resonance formula, Eq. (4), and then compared with the cross section computed from the multiresonance formula, Eq. (3). The difference in the magnitude of the cross section is a measure, at least formally, of the effect the presence of one resonance has on another. This difference in the worst case for xenon (resonance 2 located in the wings of resonance 3) was at most 5% in the region of the resonance. Of course a test like this cannot determine whether or not two resonances interact; it is only a measure of consistency.

[30]The slit width varied from 3.2 meV at 500 Å to 2.2 meV at 600 Å.

[31]The choice is somewhat arbitrary since either resonance 34 or 35 has an effective quantum number that is appropriate for the fourth member of this series.

[32]M. E. Levy and R. E. Huffman, Appl. Opt. 9, 41 (1970).